Using a Sky Projection to Evaluate Pseudorange Multipath and to Improve the Differential Pseudorange Position

Dana G. Hynes
System Test Group, NovAtel Inc.

BIOGRAPHY

Dana Hynes has been creating software for data acquisition and processing since 1975. In 1984 he began developing real time code for Transit receivers and then for GPS receivers in 1985. Since 1995 Dana has been a member of the System Test Group at NovAtel Inc providing solutions for data logging and post processing.

ABSTRACT

In order to understand the nature of the pseudorange distortions seen in GPS receiver test results, software has been developed that takes statistical results from the measurements of one or two receivers and maps them against the sky to create polar plot images. One statistic, the standard deviation of the code minus carrier, can be used to create a picture of the pseudorange distortion – usually multipath – from a single receiver. This makes it useful for imaging the code distortion pattern of a single stationary antenna.

The first part of this paper describes the method of creating the pseudorange multipath sky map and how it illustrates the way local site reflectors, the environment, antenna design and antenna location affect measurements.

The second part of this paper explores a method that uses this multipath sky map to improve the performance of a differential base station. Since the base receiver picture showed a repeatable image it seemed likely that not using data from areas of high pseudorange multipath would improve the accuracy of the rover position. The elevation cut-off for both receivers was set to the standard 15-degrees. Increasing amounts of "distortion cut-off" was applied to remove data from the areas of the image that showed higher pseudorange multipath. This experiment showed that a 15% improvement in the differential pseudorange position of the rover receiver could be achieved.

INTRODUCTION

System testing at NovAtel includes checking the quality of the range measurements at a fixed site by performing single and two card tests to produce both zero and short baseline results. This allows the checking of many classic GPS statistics such as double difference pseudorange and double difference phase. Testing showed the expected performance when the unit under test was compared against a control but the absolute maximums of the PRN specific statistics would often be large enough to require individual manual investigation.

It was noticed that most but not all of these large statistical deviations were in the same approximate area of the sky. It was also observed that the statistics plotted against time repeated every sidereal day but over the weeks statistics would change, mostly shifted by time but not always. The environment, especially rain and snow, was also recognized as another contributor to inconsistent test results.

It was hoped that by mapping the statistics against the sky we would better understand how the environment was affecting the test results and that we could eliminate the very tedious manual data processing.

METHOD OF CALCULATION

The first step in plotting statistics against the sky is to divide the hemisphere of the sky into a simple grid projection of statistical cells. This effort was made easier by the extensive use of C++ objects. When a statistic is generated from the range measurement data, it is put into the cell that encompasses the current azimuth and elevation of the associated PRN. This is done for all satellites that pass though the cell. When all data has been processed, the mean of the observations for each sky cell is calculated. By looking at the statistical cells as

pixels, where different means are given different colours, the statistics can be viewed as an image.

All data was collected on NovAtel Narrow Correlator® tracking technology dual frequency receivers with the antennae located on the flat, reflector free, metal roof of the NovAtel building (Figure 1). A hill to the northeast can be seen in the background. This man-made slope has a chain-link fence running along the top of the ridge.

Figure 1: Roof of building

CODE MINUS CARRIER (CMC)

An interesting GPS statistic can be generated by differencing the pseudorange code and the carrier phase from a single satellite to create the value known as code minus carrier (CMC). Using the data of only one receiver gives measurements at a point in space unlike the diffuse statistics generated by multiple antenna combinations. As an instrument for showing multipath it has been demonstrated that a CMC waveform with a periodic nature is most likely experiencing multipath interference [1]. The distortions may be from other causes than multipath but any repeatable interference to the signal is interesting to note. Since the measurement error of the pseudorange delay lock loop correlator is about 1000 times larger than the phase lock loop [2] the code minus carrier measurement is primarily an indication of pseudorange variation. The carrier to noise value could also have been used as an indicator of signal variance but the independently measured code and carrier is more immune to signal strength problems.

In an ideal radio-ranging world the CMC measurements would be a flat line, indicating a change of code and phase by the same amount over time thus any variation of the CMC from zero is considered a distortion of the signal.

Figure 2 shows the code minus carrier in meters of two satellites, PRN 13 in blue and PRN 24 in red, plotted for the five hours that they were in view. This data was part of a 24-hour set collected on a dry day with a choke ring patch antenna mounted directly on the roof.

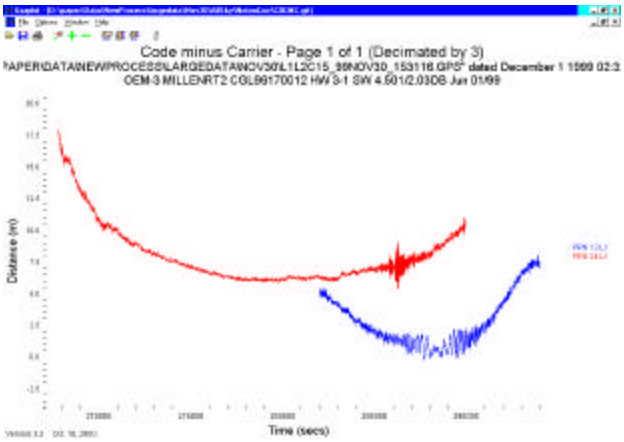

Figure 2: Code minus carrier

The distortions that start at the four hour mark are when the satellites are in the direction of the hill at about 28 degrees elevation.

The larger variations on the ends are when the satellite is close to the horizon and there is an increase in the number of possible reflectors, and increased atmospheric distortion.

The "bathtub" distortion of the code minus carrier in Figure 2 is caused by ionospheric divergence, which can be removed if two frequencies are available. The ionospheric divergence for L1 can be calculated by the following formula.

Ionospheric Delay = (L2 phase-L1 phase) / (Gamma-1)

Where:

Gamma = (L1 frequency/L2 frequency) ^{2}

Figure 3 shows the same data with ionospheric divergence removed.

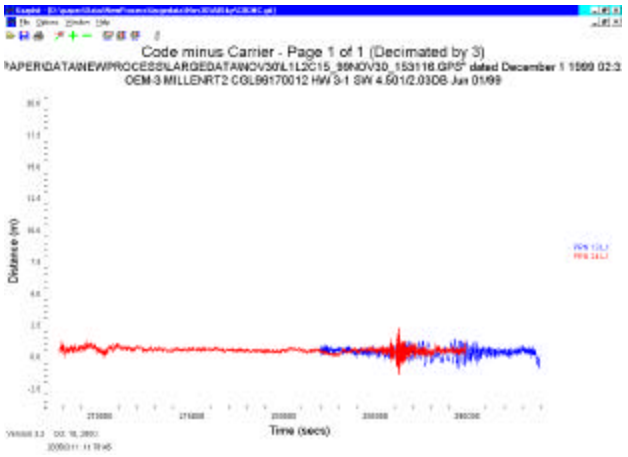

Figure 3: Code minus carrier with ionospheric divergence removed

CMC STANDARD DEVIATION (CMC SD)

Because we want to look at the amount the code minus carrier is changing when plotted against the sky the CMC standard deviation (CMC SD) is calculated. Since it is possible that more than one PRN can be in a cell at a time a CMC SD statistic is maintained separately for each satellite. When the satellite leaves the sky cell or if tracking is lost, the CMC SD of the satellite statistic is added to the appropriate statistical sky cell. In the final polar plot image each sky cell contains the average of all the standard deviations of all the satellites that have passed though it. To do this procedure reliably requires checking for minimum samples, bridging phase lock breaks, and other discontinuities.

The size of the cell chosen depends on the type of information desired. A small cell size will show the satellite tracks and the larger cell will give a better impression of where the measurement distortions are. A larger cell size will also pass through lower frequency distortions increasing the amount of variation calculated. The method of dividing the sky into cells, or projection, can also lead to a difference in the lowest frequency of distortion that can be detected. For example the grid array projection, chosen for its simplicity, has large cells on the horizon and small cells at the zenith. The default cell size used is 2 degrees elevation by 5 degrees azimuth.

Consistent results can be best achieved by collecting 24-hour data sets. This overcomes the problem of collecting data at different times of the day and permits comparison of different data sets started at different times of the day. It also makes full use of the constellation of satellites available to obtain maximum coverage in the sky plots. A measurement period of 10 seconds has proved to be sufficient for tracking the relatively slow changing statistics.

THE SKY PLOT

Figure 4 shows the CMC SD plotted against the sky using the complete data set. North is at the top of the polar plot, the east is on the right, south is at the bottom and left is the west. The horizon is around the rim and the zenith is in the centre. White is where no satellites have gone. The prominent hole in the upper centre is due to the fact that satellites never go over the poles. This site has been plotted many times over and this image has always appeared when the environmental conditions are dry.

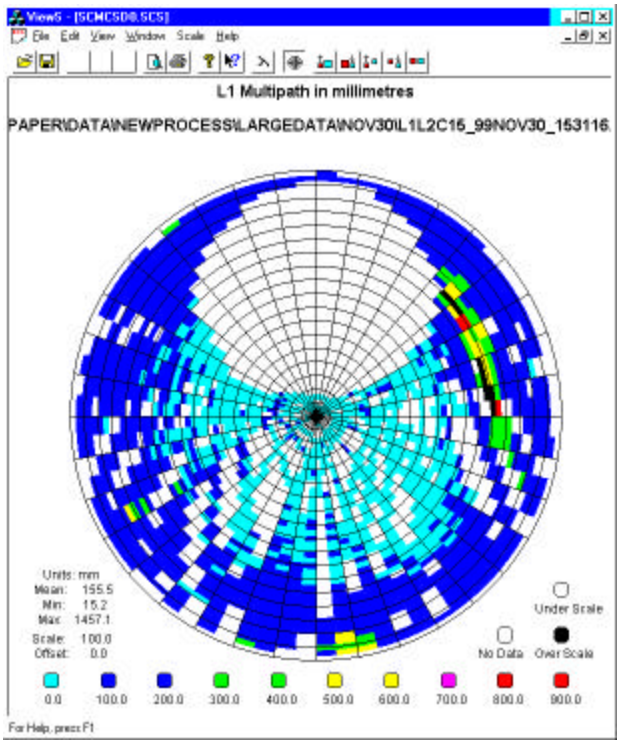

Figure 4: CMC SD mapped against the sky

The main feature of the image in Figure 4 is the bump in the northeast in the upper right hand part of the plot. The bump appears in the same location in the plot even when the antenna is moved several meters or to the side of the building. This indicates that the source of interference is not local to the roof. We believe that the source of the interference is a hill to the northeast of the building (visible in the photograph of Figure 1). It is important to note that the image does not indicate where the multipath is coming from but rather where the satellite is when its signal is being interfered with.

PRNS 13 AND 24 AGAINST THE SKY

Figure 5 shows the paths of the two satellites shown as a time series in Figure 2. The track of PRN 13 glances off the hill in the northeast quadrant while PRN 24 rises from the south to nearly straight up before coming down sharply through the hill area to the east.

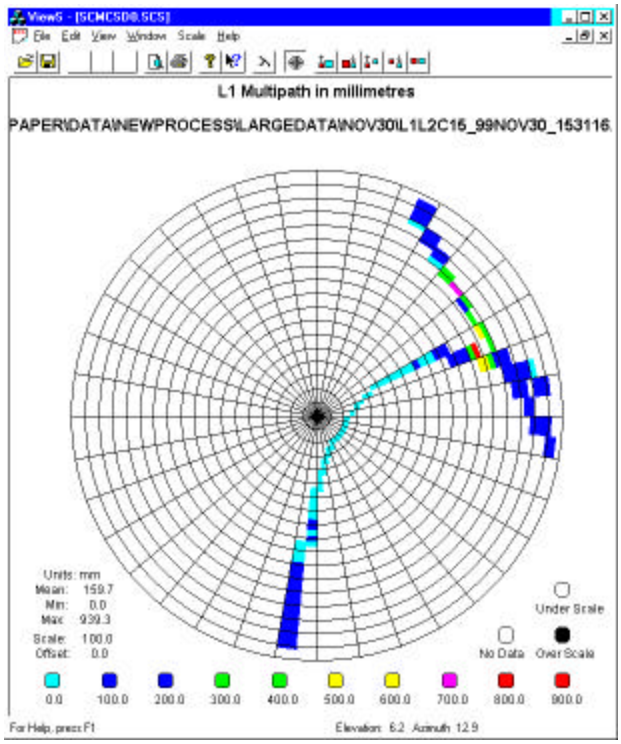

Figure 5: PRNs 13 and 24 CMC SD against the sky

THE HILL AREA AGAINST TIME

To show that the large standard deviations in the image in Figure 4 correlate with the large standard deviations shown in Figure 3 the data is re-processed with only the measurements in the area of the hill being plotted. Comparing Figure 6 to Figure 3 shows that only the portions containing large CMC deviations remain. This often repeated experiment illustrates that the distortion is not a pattern generated by a particular PRN every 24 hours but rather a distortion pattern driven by the location in the sky.

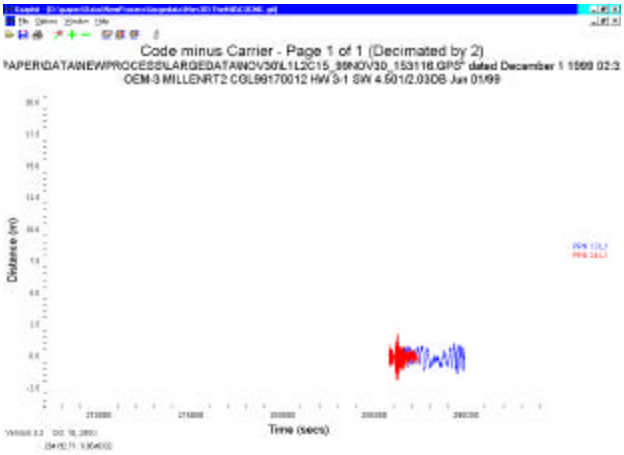

Figure 6: The hill area against time

HIGH RESOLUTION IMAGES

Figure 7 shows the detail of the site by combining data from many data sets spaced over 18 months plotted with a cell size of 1 degree elevation by 2 degrees azimuth. Besides the hill, there is another interesting artifact in Figure 7, a line that crosses the satellite tracks from the southwest and ends near straight up. The cause is not immediately apparent when looking at the roof and the surrounding area. It is not a GPS satellite since its trajectory leads to the hole over the North Pole.

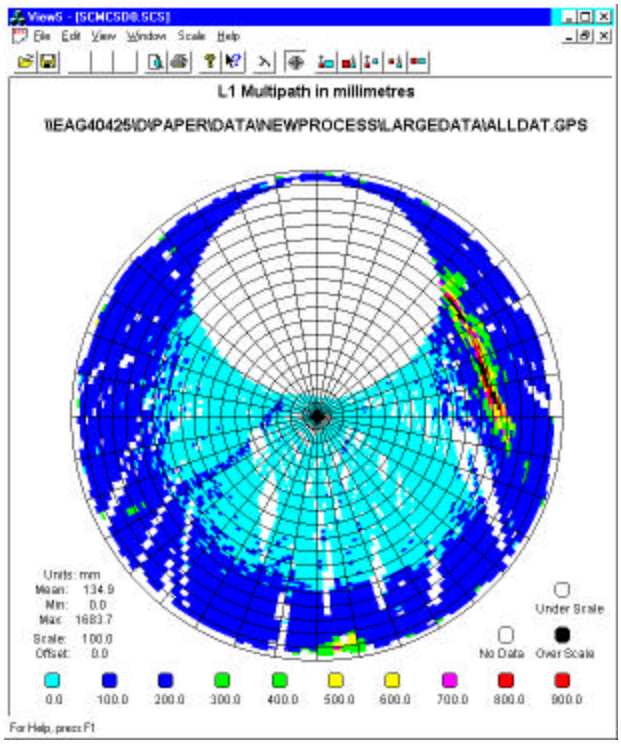

Figure 7: High resolution L1

The incomplete track in Figure 7 that can be seen in the southeast at 105 degrees azimuth by 30 degrees elevation is evidence of the use of a twenty-two hour data set.

Figure 8 shows the L2 data, which has a much higher multipath level due to the lower signal strength and tracking differences. Note that the artifact shown in Figure 7 is not present indicating that the effect is frequency dependent.

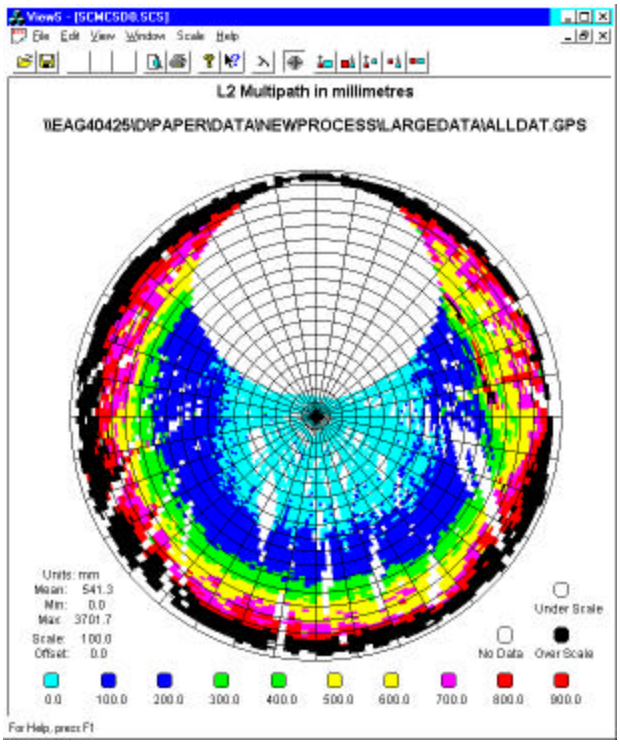

Figure 8: High resolution L2

THE EFFECT OF ANTENNA DESIGN

Located within 5 meters of the choke ring antenna shown in Figure 4 is a non-choke ring patch antenna mounted at the same 1 foot height. The CMC SD for the non-choke antenna shown in Figure 9 illustrates that although the mean has increased from 155 mm to 175 mm the pattern remains the same in both images.

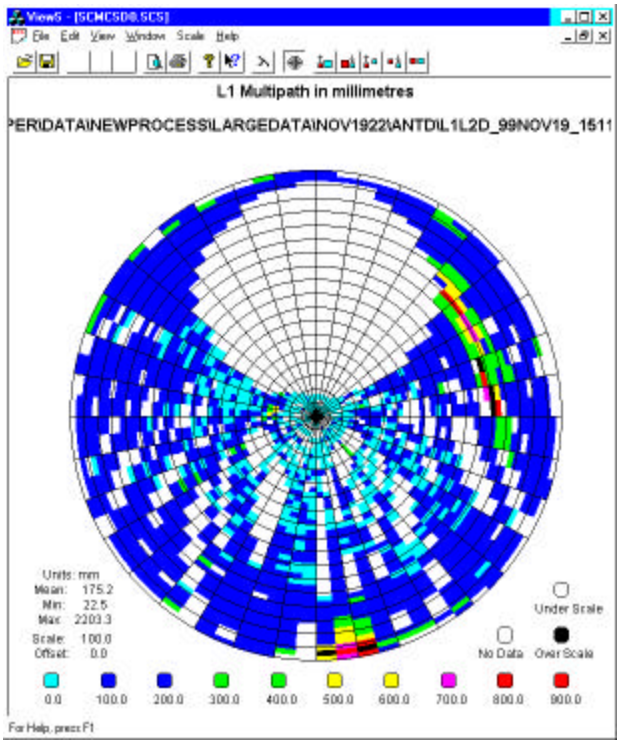

Figure 9: Non-choke ring antenna

THE CMC SD SKY PLOT WITH IONOSPHERIC DIVERGENCE

The code minus carrier does not have to have the ionospheric divergence removed to create a useful sky plot. Figure 10 has the same data that was used in Figure 4 without the ionospheric delay correction formula being applied. The uncorrected image is best when smaller cell sizes are used to reduce the low frequency effect of the "bathtub" shaped ionospheric divergence.

The main change in this image as compared to the ionospheric delay corrected image in Figure 4 is the increase in CMC SD variation at lower elevations. Note also that some of the satellite tracks at higher elevations can now be seen in a darker shade of blue. These long higher variance tracks will appear in the sky when the ionospheric delay correction has not been applied due to the day to night variation of the ionosphere.

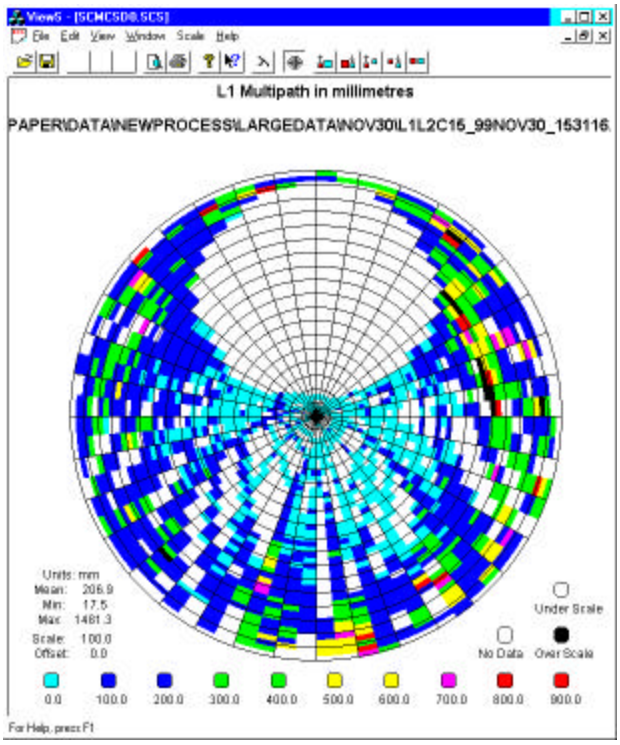

Figure 10: CMC SD with ionospheric divergence

THE EFFECT OF HEIGHT

Figure 11 and Figure 12 show the same type of choke ring antenna as in Figure 4 mounted higher at 3 and 5 foot heights. While the multipath is low when the antenna is mounted low, the reflective metal roof adversely affects the CMC SD when the antenna is mounted higher. The mean of the CMC SD increases from 155 mm for the antenna mounted at a 1 ft height, to 264 mm for the 3 foot height, and then 334 mm for the 5 foot. Of course if there were a large reflector in the area it would probably be better to put the antenna above the height of the reflector.

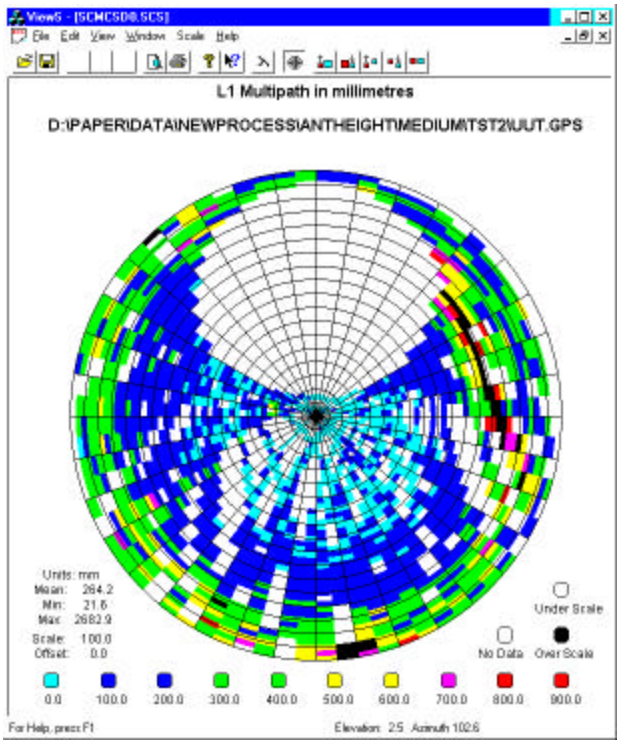

Figure 11: Medium height

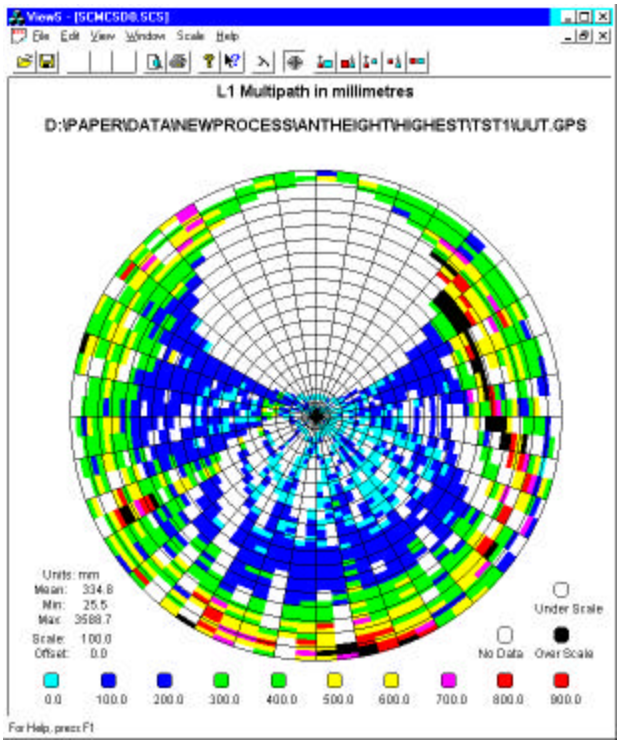

Figure 12: Highest

THE EFFECT OF CELL SIZE

Figure 13 is the same data as Figure 12 but processed with cell sizes of 5 degrees elevation and 10 degrees azimuth. The mean of the CMC SD has increased from 334 mm to 454 mm due to the larger cell size allowing the lower frequencies through.

Note that the antenna is now above the level of the lip of the roof and the CMC SD is lower between 0 to 5 degrees than it is between 5 to 10 degrees. This is mainly because the choke ring design is best at rejecting multipath at low angles of incidence [3]. The geometry between the satellite on the horizon, the antenna, and the surrounding objects also contributes to a lower variance in the CMC SD at the lower elevations.

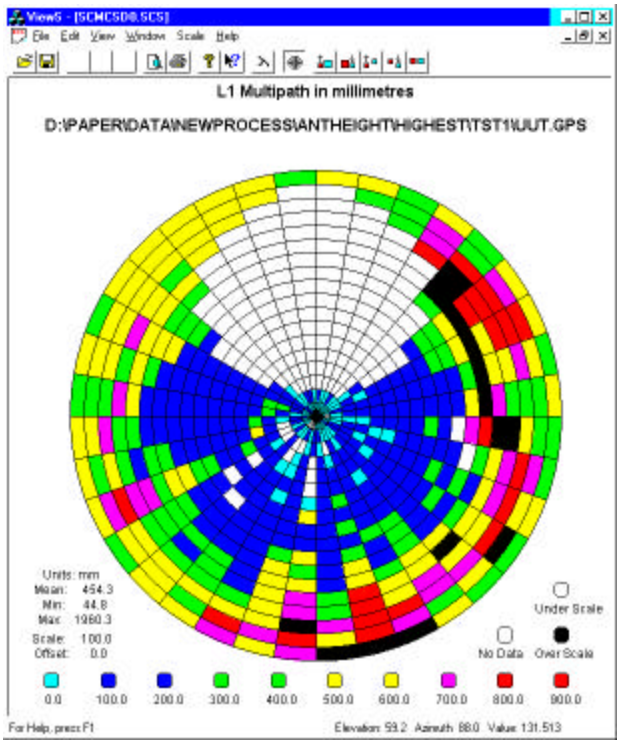

Figure 13: Low resolution highest

THE EFFECT OF LOCATION ON THE ROOF

Figure 14 shows the effect of mounting the same height choke ring antenna used in Figure 13 on the southwest side of the roof. The antenna is now farther away from the hill in the northeast and as such the amount of multipath from that direction has decreased. The parking lot below to the southwest is very prominent in this image.

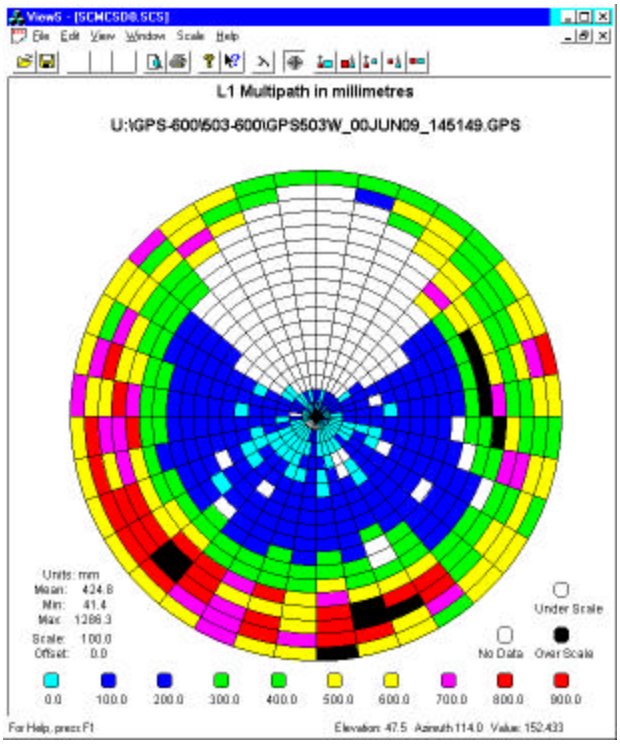

Figure 14: Southwest side of roof

THE EFFECT OF RAIN

Figure 15 shows how rain causes the multipath from the direction of the hill to disappear. This plot was generated by taking from the sky plot the average of the CMC SD of all azimuth angles for each elevation. There were three sets of data collected on the side of the building with a NovAtel 600 antenna where in the third set (green line) it rained.

Note the decrease in multipath from the hill in the third data set at the 28 degrees elevation angle. It is not known if this is due to the reflectors being dampened by the water or by the rain itself attenuating the reflected signal.

The repeatability of the site is demonstrated in Figure 15 by how well data sets 1 and 2 (red and blue lines) overlay each over. This plot also shows the reduction of the variance of the CMC SD at the horizon.

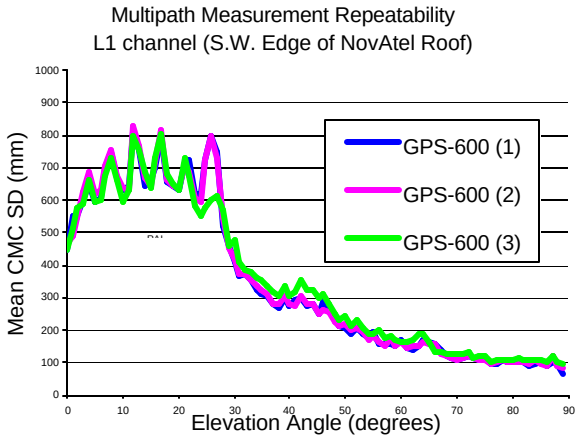

Figure 15:The effects of rain

The CMC SD in Figure 15 also shows a periodic pattern between 0 and 30 degrees that appears with all types of antennae mounted at higher levels anywhere on the NovAtel roof. These equal periods might be a characteristic of the CMC SD pattern of a flat reflective metal roof. These equal periods do not appear in data collected on the roof of the two-story house shown in Figure 17.

PLOTS FROM A TWO-STORY HOUSE

The performances of the antennas change when used at a different site. The following four figures are from the two antennas mounted on top of a two-story house that has a clear view of the sky in all directions. The house itself is made of materials that are somewhat transparent to the GPS signals.

Figure 16: Choke ring antenna on a residential house

The residential choke ring antenna in Figure 16 is shown in Figure 17 to have a mean CMC SD of 407 mm. This is better than the 454 mm in Figure 13 of the same choke ring antenna mounted at the five foot level at NovAtel.

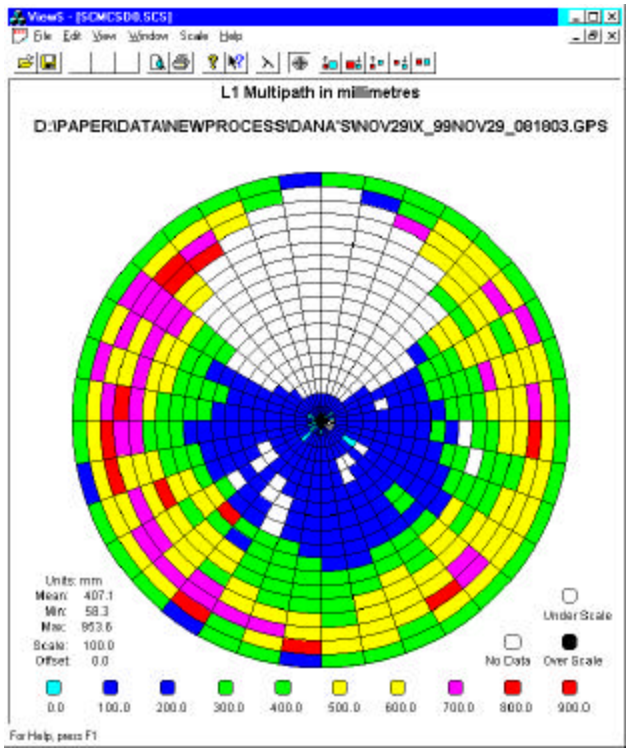

Figure 17: CMC SD of residential choke ring antenna

The choke ring antenna in Figure 17 clearly shows a reduction of variance on the horizon. The non-choke antenna shown in Figure 18 is mounted directly to the south of the choke antenna. It shows the lesser effect of satellite geometry as a contributor to the reduction of variance for satellites low on the horizon. The CMC SD mean in Figure 19 of 713 mm for the residential non-choke antenna is much higher than the 407 mm of the choke ring antenna on the same roof.

Figure 18: Residential non-choke ring antenna

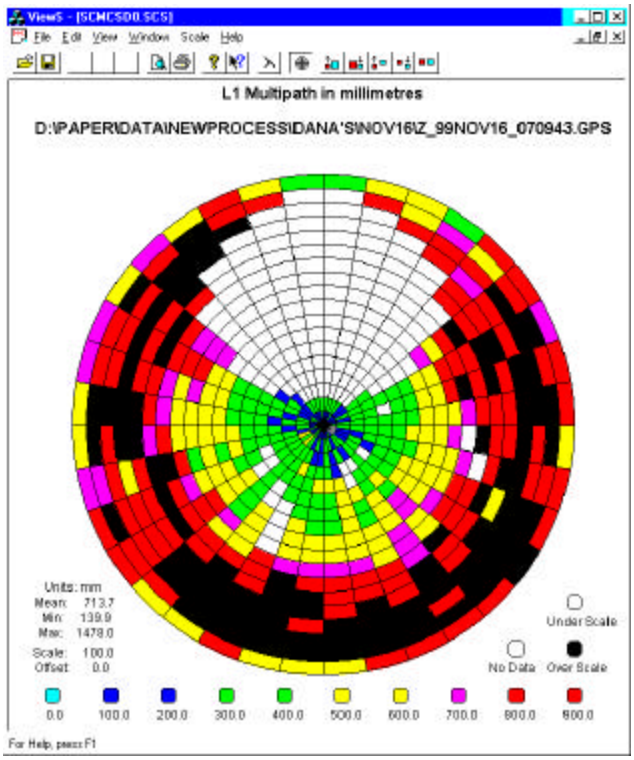

Figure 19: CMC SD of the residential non-choke ring antenna

IMPROVING THE DIFFERENTIAL POSITION

If the areas with high code minus carrier numbers in the sky plot indicate an area that would usually produce poor pseudorange measurements, then it seemed likely that by removing those areas the end result would improve.

It was decided to test this hypothesis by taking a standard medium baseline (15.5 km) two-card 24-hour data set and post processing it as a differentially corrected pseudorange position. The base was a patch choke ring antenna 1 foot above the NovAtel roof and the rover was the patch antenna shown in Figure 18. The cut-off elevation was set to 15 degrees for both base and rover. Figure 20 shows that with no filtering the average 3D position error was 60 cm. It also shows that without filtering the resulting position is given a 3D standard deviation of 53 cm. Filtering by removing data with code minus carrier standard deviation greater than 1 metre still has no effect in position accuracy since there was no distortion that large at the base station. When a filter of 800 cm was applied the average error decreased to 53 cm. A filtering of 600 and 500 cm produced a slightly better improvement of 52 cm and then the position error increases due to the removal of too many satellites from the data. For this site it appears that a conservative CMC SD cut off of 750 mm gives a satisfactory position improvement of 7 cm to produce a matching calculated standard deviation of 53 cm. This algorithm will work in

real time as well as post due to the repeatable nature of the multipath image.

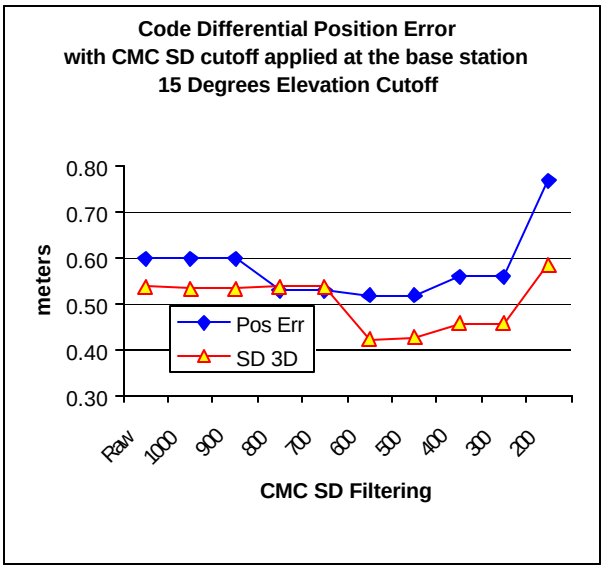

Figure 20: Pseudorange position improvement

CONCLUSIONS

Plotting GPS quality numbers against the sky, such as code minus carrier standard deviation, provides a useful tool in evaluating GPS signal distortion. This method can be applied in any application where the location and range of the RF transmitter is known.

If there are no reflectors or obstructions in the immediate area the antenna height (HI) is best kept to a minimum. It also has been shown that rain can reduce multipath. For site evaluation GPS data is best gathered with the equipment that will be used at the site when it is up and running.

If an antenna is at a fixed site, there is a repeatable nature of the code minus carrier standard deviation as mapped against the sky. This provides a means to weight the accuracy of the data that is used in the solution computed.

The software was originally created with the idea to provide a software test for tracking loops that produced repeatable absolute numbers with live data. Our knowledge of the sources of the distortions has greatly improved and data is now easier to process. We have found however, that the use of control receivers gives the best indication of test set-up and/or environmentally induced errors.

AREAS OF FUTURE STUDY

Figure 15 showed that there are mo re details in the sky plot than can be seen with the discrete colour pallet currently used. A smooth rainbow spectrum representing the CMC SD values would bring out this detail on the sky maps.

There are other methods of reducing multipath such as correlator design that have an interesting effect on the CMC SD plots generated.

The CMC SD cells could be filtered by other means such as frequency to provide information on the amount of multipath delay in the signal.

There are interesting things to see in the sky plots of other statistics such as C/No, lock times and double difference phase.

With the addition of roll, pitch and azimuth information it may be possible to apply this method to dynamic vehicles. This may work best with aircraft when they are away from ground since the airframe represents a fixed site.

If the multipath is coming from the hill as suspected, would placing a simple GPS radio frequency block between the antenna and the hill remove that bump of variation in the CMC SD sky plot? A small RF absorber blocking 0 to 7 degrees in elevation and 40 to 100 degrees in azimuth could make this good site even better.

ACKNOWLEDGEMENTS

The author would like to thank Jonathan Auld, Waldemar Kunysz, Pat Fenton, Janet Neumann, and Jim Rooney for their help and advice.

REFERENCES

1. Leick, Alfred, “GPS Satellite Surveying, 2nd Edition”, Wiley – Interscience, 1995, Pages 311-316.

2. B. W. Parkinson, “Introduction And Heritage Of Navstar”, Global Positioning System: Theory and Applications, Volume I, Progress in Astronautics and Aeronautics, Volume 163, American Institute of Aeronautics and Astronautics, Inc., Page 18, Chapter 1.

3. Elliott D. Kaplan, “Understanding GPS Principles and Applications”, Artech House Publishers, 1996, Page 259.